



ALMA MATER STUDIORUM
UNIVERSITÀ DI BOLOGNA

ARCHIVIO ISTITUZIONALE
DELLA RICERCA

Alma Mater Studiorum Università di Bologna Archivio istituzionale della ricerca

Perfluorooctane sulfonic acid, a persistent organic pollutant, inhibits iodide accumulation by thyroid follicular cells in vitro

This is the final peer-reviewed author's accepted manuscript (postprint) of the following publication:

Published Version:

Conti A., Strazzeri C., Rhoden K.J. (2020). Perfluorooctane sulfonic acid, a persistent organic pollutant, inhibits iodide accumulation by thyroid follicular cells in vitro. *MOLECULAR AND CELLULAR ENDOCRINOLOGY*, 515, 110922-110922 [10.1016/j.mce.2020.110922].

Availability:

This version is available at: <https://hdl.handle.net/11585/801705> since: 2021-02-19

Published:

DOI: <http://doi.org/10.1016/j.mce.2020.110922>

Terms of use:

Some rights reserved. The terms and conditions for the reuse of this version of the manuscript are specified in the publishing policy. For all terms of use and more information see the publisher's website.

This item was downloaded from IRIS Università di Bologna (<https://cris.unibo.it/>).
When citing, please refer to the published version.

(Article begins on next page)

This is the accepted manuscript of:

Conti A, Strazzeri C, Rhoden KJ. Perfluorooctane sulfonic acid, a persistent organic pollutant, inhibits iodide accumulation by thyroid follicular cells in vitro. *Mol Cell Endocrinol.* 2020 Sep 15;515:110922

Final peer reviewed version available at <https://doi.org/10.1016/j.mce.2020.110922>

Rights / License:

The terms and conditions for the reuse of this version of the manuscript are specified in the publishing policy. For all terms of use and more information see the publisher's website.

This item was downloaded from IRIS Università di Bologna (<https://cris.unibo.it/>)

When citing, please refer to the published version.

1 **Perfluorooctane sulfonic acid, a persistent organic pollutant, inhibits iodide**
2 **accumulation by thyroid follicular cells *in vitro***

3

4 Amalia Conti ^a, Chiara Strazzeri ^b, and Kerry J. Rhoden ^c

5

6 ^a Department of Medical and Surgical Sciences (DIMEC), University of Bologna, S. Orsola-
7 Malpighi Hospital, via Massarenti 9, Bologna 40138, Italy; amalia.conti2@unibo.it

8 ^b Department of Medical and Surgical Sciences (DIMEC), University of Bologna, S. Orsola-
9 Malpighi Hospital, via Massarenti 9, Bologna 40138, Italy; chiara.strazzeri@studio.unibo.it

10 ^c Department of Medical and Surgical Sciences (DIMEC), Health Sciences & Technologies
11 Interdepartmental Center for Industrial Research (CIRI SDV), University of Bologna, S.
12 Orsola-Malpighi Hospital, via Massarenti 9, Bologna 40138, Italy; kerry.rhoden@unibo.it

13

14 **Corresponding author**

15 Kerry J. Rhoden, UO Genetica Medica, Policlinico S. Orsola-Malpighi pad 11, via
16 Massarenti 9, Bologna 40138, Italy; kerry.rhoden@unibo.it

17

18 **Declarations of interest:** none

19

20

21

22 **Abstract**

23 Poly- and perfluoroalkyl substances (PFAS) are a class of endocrine disrupting chemicals
24 (EDCs) reported to alter thyroid function. Iodide uptake by thyroid follicular cells, an early
25 step in the synthesis of thyroid hormones, is a potential target for thyroid disruption by
26 EDCs. The aim of the present study was to evaluate the acute effects of perfluorooctane
27 sulfonic acid (PFOS) and perfluorooctane carboxylic acid (PFOA), two of the most
28 abundant PFAS in the environment, on iodide transport by thyroid follicular cells *in vitro*.
29 Dynamic changes in intracellular iodide concentration were monitored by live cell imaging
30 using YFP-H148Q/I152, a genetically encoded fluorescent iodide biosensor. PFOS, but
31 not PFOA, acutely and reversibly inhibited iodide accumulation by FRTL-5 thyrocytes, as
32 well as by HEK-293 cells transiently expressing the Sodium Iodide Symporter (NIS). PFOS
33 prevented NIS-mediated iodide uptake and reduced intracellular iodide concentration in
34 iodide-containing cells, mimicking the effect of the NIS inhibitor perchlorate. PFOS did not
35 affect iodide efflux from thyroid cells. The results of this study suggest that disruption of
36 iodide homeostasis in thyroid cells may be a potential mechanism for anti-thyroid health
37 effects of PFOS. The study also confirms the utility of the YFP-H148Q/I152 cell-based
38 assay to screen environmental PFAS, and other EDCs, for anti-thyroid activity.

39

40 **Key words:** endocrine chemical disruptor, thyroid follicular cell, iodide, Sodium Iodide
41 Symporter, poly- and perfluoroalkyl substances (PFAS), perfluorooctane sulfonic acid
42 (PFOS)

43

44 **1. Introduction**

45 Per- and polyfluoroalkyl substances (PFAS) are a group of man-made chemicals that have
46 raised world-wide concern as persistent organic pollutants that threaten ecosystems and
47 human health (ITRC, 2018; Wang et al., 2017). Thanks to their unique physicochemical
48 properties - resistance to oil, water, heat and degradation - PFAS have been extensively
49 used in manufacturing processes since the 1950's. They are present in a vast array of
50 industrial and consumer products, including fire-fighting foams, hydraulic systems,
51 electronic components, building materials, paints, textiles, food packaging, non-stick
52 cookware, cleaning agents and cosmetics, among others. At least 3000 PFAS are on the
53 global market (KEMI, 2015), of which perfluorooctane sulfonic acid (PFOS) and
54 perfluorooctanoic acid (PFOA) have historically been the most widely used.

55 The same physicochemical properties that underlie their industrial and consumer utility
56 have also led to the ubiquitous and persistent occurrence of PFAS in the environment and
57 biota. PFAS are bioaccumulated thanks to their ability to interact with both phospholipids
58 and proteins (Ng and Hungerbühler, 2014). Partitioning to cell membranes, and
59 noncovalent binding to transporters and serum proteins, accounts for the broad tissue
60 distribution of PFAS in wildlife and man, and to their slow elimination from the body (Ng
61 and Hungerbühler, 2014). Indeed, PFOS and PFOA have extremely long serum
62 elimination half-lives in man of 4.8 and 3.5 years, respectively (Olsen et al., 2007).

63 Human exposure to PFAS has been linked to a variety of health effects, including altered
64 hormone and cholesterol levels, impaired pre- and post-natal development, reproductive
65 dysfunction, immunotoxicity, liver damage, and certain types of cancer (EFSA, 2018;
66 USEPA, 2016). The World Health Organization has included both PFOS and PFOA in its
67 assessment of endocrine disrupting chemicals (EDCs) (WHO, 2013). Epidemiologic and
68 laboratory studies have reported thyroid disruption by both compounds, although not

69 consistently (Coperchini et al., 2017; EFSA, 2018; USEPA, 2016). Reported effects are
70 highly heterogeneous, and may involve different steps in the synthesis, metabolism,
71 clearance and action of thyroid hormones. Given that PFAS and PFOA exist in the
72 environment in their anionic form, it is reasonable to hypothesize that, in the body, these
73 chemicals may interfere with the homeostasis of physiological anions, and in the case of
74 the thyroid gland, with that of iodide.

75 Iodine is necessary for the synthesis of thyroid hormones, thyroxine (T4) and
76 triiodothyronine (T3). The thyroid gland concentrates circulating iodide thanks to the
77 Sodium Iodide Symporter (NIS; SLC5A5), a secondary active transporter present on the
78 basolateral surface of thyroid follicular cells (Portulano et al., 2014). Iodide uptake by NIS
79 is followed by diffusion across the apical membrane into the lumen of thyroid follicles for
80 incorporation into thyroglobulin, the precursor of thyroid hormones. Using a high
81 throughput screening assay, the U.S. EPA's Endocrine Disruptor Screening Program
82 (EDSP) identified PFOS as a NIS inhibitor in HEK293T cells expressing human NIS and
83 FRTL-5 thyroid cells (Buckalew et al., 2020; Wang et al., 2019, 2018). The aim of the
84 present study was to evaluate the effect of PFOS and PFOA on intracellular iodide
85 concentration in thyroid cells *in vitro* in order to address impairment of iodide homeostasis
86 as a potential mechanism for the anti-thyroid effect of PFAS.

87 **2. Materials and Methods**

88 **2.1. Materials**

89 Chemicals and reagents, unless otherwise specified, were obtained from Sigma-Aldrich,
90 including PFOS (catalog #77283) and PFOA (catalog # 71468). Cell culture media, unless
91 otherwise specified, were obtained from Euroclone (Italy). FRTL-5 cells were kindly
92 provided by Dr. F. Curcio and Dr. F.S. Ambesi-Impiombato of the University of Udine
93 (Italy). Plasmids pcDNA3.1-YFP-H148Q/I152L (Galiotta et al., 2001) and pcDNA3-hNIS
94 (Smanik et al., 1996) were kindly provided by Dr. LGV Galiotta (TIGEM, Italy) and Dr. S.M.
95 Jhiang (Ohio State University), respectively. Other materials and their sources are
96 described in the relevant Methods section.

97 **2.2. Cell culture and transfection**

98 FRTL-5 normal rat thyroid follicular cells were cultured in Coon's modified nutrient mixture
99 F-12 Ham (Sigma-Aldrich) supplemented with 5% newborn calf serum, 1 mg/ml insulin, 3.6
100 ng/ml hydrocortisone, 5 mg/ml apotransferrin, 10 ng/ml gly-his-lys acetate, 10 ng/ml
101 somatostatin, 1 mU/ml thyroid-stimulating hormone (TSH), 100 U/ml penicillin and 100
102 mg/ml streptomycin (Ambesi-Impiombato et al., 1980). HEK-293 cells were cultured in
103 Dulbecco's modified Eagle medium (DMEM) supplemented with 10% fetal bovine serum
104 (FBS), 2 mM glutamine, 100 U/ml penicillin and 100 mg/ml streptomycin. All cells were
105 maintained at 37°C in humidified air containing 5% CO₂.

106 A clonal population of FRTL-5 cells with stable expression of YFP-H148Q/I152L (referred
107 to hereafter as FRTL5-YFP) was previously generated and used to monitor intracellular
108 iodide (Rhoden et al., 2008, 2007). HEK-293 cells were transiently co-transfected with
109 pcDNA3.1-YFP-H148Q/I152L and pcDNA3-hNIS, using Lipofectamine 3000
110 (ThermoFisher Scientific) according to manufacturer's instructions. Transfection efficiency,

111 estimated as the proportion of fluorescent cells 48h post-transfection, was typically >80%.
112 hNIS expression in HEK-293 cells was confirmed by Western blotting using anti-
113 hNIS(KELE) antibody.

114 **2.3. Dynamic monitoring of intracellular iodide concentration**

115 Intracellular iodide concentration was monitored by microscopic live cell imaging with YFP-
116 H148Q/I152L, a fluorescent genetically-encoded iodide biosensor, as previously described
117 (Cianchetta et al., 2010; Di Bernardo et al., 2011; Rhoden et al., 2007, 2008). Cells were
118 sub-cultured on 25 mm diameter round glass coverslips in 6-well culture dishes.
119 Coverslips were mounted on a thermostatically-controlled RC-21BR imaging chamber
120 connected to a VC-8 perfusion valve control system and TC-344B temperature controller
121 (Warner Instruments). Fluorescence intensity (excitation 500 ± 12.5 nm, emission 545 ± 17.5
122 nm) was monitored with an Axiovert 200 inverted fluorescence microscope (Carl Zeiss)
123 equipped with a 40x oil immersion objective and Lambda 10C optical filter changer (Sutter
124 Instrument Company; Crisel Instruments, Rome, Italy). Image acquisition was performed
125 with a Coolsnap HQ² CCD (Photometrics; Crisel Instruments, Rome, Italy) and Metafluor
126 Imaging Software (Molecular Devices; Crisel Instruments, Rome, Italy). Images were
127 acquired with an exposure of 25 ms every 10 seconds.

128 Imaging chambers were perfused continuously with a serum-free balanced salt solution
129 (BSS) composed of 137 mM NaCl, 2.7 mM KCl, 0.7 mM CaCl₂, 1.1 mM MgCl₂, 1.5 mM
130 KH₂PO₄, 8.1 mM Na₂HPO₄ and 10 mM glucose (pH 7.4) at 37°C. Baseline fluorescence
131 was recorded for at least 5 min at the beginning of each experiment, after which cells were
132 exposed to 10 μM NaI in order to induce iodide accumulation. The effects of test reagents
133 (PFOS, PFOA, NaClO₄, or ouabain) on intracellular iodide concentration were evaluated
134 according to one or more of the following protocols: Protocol I, 2 min pre-treatment +/- test

135 reagents, followed by 10 min exposure to 10 μ M NaI +/- test reagents; Protocol II, 10 min
136 exposure to 10 μ M NaI, followed by 10 min exposure to 10 μ M NaI +/- test reagents;
137 Protocol III, 10 min exposure to 10 μ M NaI, followed by 10 min exposure to BSS +/- test
138 reagents. Stock solutions of test reagents were prepared in distilled water and diluted
139 appropriately in BSS.

140 Intracellular iodide concentration was quantified from iodide-induced changes in cellular
141 YFP-H148Q/I152L fluorescence, as described previously (Cianchetta et al., 2010; Di
142 Bernardo et al., 2011; Rhoden et al., 2008, 2007). Average fluorescence intensity was
143 quantified within a region-of-interest (ROI) containing 20-50 cells, paying careful attention
144 to select an ROI without cell loss during the entire duration of the experiment. Background
145 fluorescence of a cell-free area was subtracted. To control for the decline in cellular
146 fluorescence over time due to photo-bleaching of the fluorophore, baseline fluorescence in
147 iodide-free BSS measured during the first 5 min of each experiment, was fit by non-linear
148 regression to a one-phase exponential decay curve. Cellular fluorescence (F) at each time
149 point of the experiment was then normalized to the corresponding best-fit value of baseline
150 fluorescence (F_0) to obtain a measure of relative fluorescence ($RF=F/F_0$). Intracellular
151 iodide concentration was calculated according to the equation $[I] = K_{0.5}(RF_{max}-RF)/(RF-$
152 $RF_{min})$ where $K_{0.5}$ is the affinity of YFP-H148Q/I152L for iodide, RF is relative fluorescence
153 at each time point during the experiment, and RF_{max} and RF_{min} represent the maximal and
154 minimal values of RF in the absence and presence of saturating iodide, respectively.
155 RF_{max} is 1, by definition, and mean values for RF_{min} (0.036) and $K_{0.5}$ (1.372 mM) were
156 determined experimentally using FRTL5-YFP cellular extracts (see section 2.4). The
157 maximal rate of iodide uptake, defined as the maximal rate of change of intracellular iodide
158 concentration ($\Delta[I]/\Delta t$), was estimated by fitting intracellular $[I]$ to a one-phase exponential
159 association equation with respect to time, and obtaining the derivative of the best fit curve.

160 The rate constant of iodide efflux was estimated by fitting intracellular $[I^-]$ to a one-phase
161 exponential decay equation with respect to time.

162 **2.4. YFP-H148Q/I152L fluorescence in cellular extracts**

163 In order to evaluate whether PFAS interfere with the ability of YFP-H148Q/I152L to detect
164 iodide, experiments we carried out using FRTL5-YFP cellular extracts. Cells were cultured
165 in T75 flasks till near confluence, detached in PBS and micro-centrifuged at 12000g for 10
166 min at 4°C. Cellular pellets were disrupted with a pestle in 10 mM HEPES pH 7 (200 μ l per
167 pellet) and passed repeatedly through a 28-gauge needle. Lysates were centrifuged, and
168 supernatants containing liberated YFP-H148Q/I152L were collected on ice. Pellets were
169 re-suspended in 10 mM HEPES pH 7, homogenized and centrifuged to recover further
170 YFP-H148Q/I152L. Samples of pooled supernatants were diluted 1:1 with HEPES 10 mM
171 pH 7 containing NaI and/or PFOS to achieve a range of final concentrations (0.1-100 mM
172 NaI, 0.1-10 mM PFOS). Replicate 10 μ l aliquots were deposited on a coverslip, and
173 fluorescence images were acquired with the same imaging station used for cellular
174 experiments. Average fluorescence intensity within a constant ROI was quantified and
175 normalized against the mean value obtained in the absence of NaI, to obtain a measure of
176 relative fluorescence ($RF=F/F_0$). The affinity of YFP-H148Q/I152L for iodide ($K_{0.5}$) was
177 defined as the concentration of NaI causing a 50% of maximal decrease in relative
178 fluorescence intensity.

179 **2.5. SDS-PAGE electrophoresis and Western blotting**

180 Cells were lysed in ice-cold buffer (50 mM Tris pH 7.4, 150 mM NaCl, 0.1% SDS, 1 %
181 Triton-X, 1 mM EDTA), supplemented with Roche cOmplete Protease Inhibitor cocktail.
182 Lysates were passed repeatedly through a 20-gauge needle on ice. Protein concentration
183 was measured colorimetrically using the DC Protein Assay (Bio-Rad) according to the

184 manufacturer's instructions. Lysates were mixed 1:1 with a modified Laemmli sample
185 buffer (125 mM Tris pH 6.8, 20% glycerol, 20% SDS 20%, 200 mM dithiothreitol, and 0.2%
186 bromophenol blue), and incubated for 30 min at 37°C. Samples (40 µg protein) were
187 subjected to SDS-PAGE electrophoresis using hand-cast 9% gels in a Mini-Protean Tetra
188 Vertical Electrophoresis Cell (Bio-Rad). Samples were transferred onto 0.2 µM
189 nitrocellulose membranes using the Trans-Blot Turbo Transfer System (Bio-Rad). For
190 Western blotting, membranes were incubated with WesternBreeze Blocker/Diluent
191 (ThermoFisher) for 1h at room temperature, primary antibody overnight at 4°C, and
192 peroxidase-conjugated secondary antibody for 1h at room temperature, with frequent
193 washing in Tris-buffered saline containing 0,1% Tween. Bound antibodies were detected
194 by enhanced chemiluminescence using WESTAR Supernova substrates (Cyanagen,
195 Bologna, Italy) and a ChemiDoc™ XRS+ Imaging System (Bio-Rad). The following
196 antibodies were used: rabbit polyclonal anti-hNIS(KELE) antibody (Tazebay et al., 2000)
197 generously provided by Dr. N. Carrasco (Yale University) and Dr. C. Portulano (formerly of
198 Albert Einstein College of Medicine, USA), mouse monoclonal anti-γ-tubulin antibody clone
199 GTU-88 (Sigma-Aldrich), goat anti-rabbit IgG-peroxidase antibody (Sigma-Aldrich), and
200 goat anti-mouse IgG-peroxidase (Sigma-Aldrich).

201 **2.6. Cytotoxicity**

202 Cell viability was assessed using a Quick Cell Proliferation Colorimetric Assay Kit Plus
203 (BioVision) based on the cleavage of water-soluble tetrazolium salt to formazan by cellular
204 mitochondrial dehydrogenase. FRTL-5 cells were exposed to PFOS or PFOA (1-100 µM)
205 for 1h, and viability was assayed according to manufacturer's instructions. Absorbance
206 was read at 450 nm using a Model 680 Microplate Reader (Bio-Rad).

207

208 **2.7. Data analysis**

209 Data analysis, including curve fitting, iodide quantification and statistical analyses, were
210 performed using Graphpad Prism Software. Data are expressed as mean values +/- SEM
211 of *n* independent experiments performed on cells from different passages. Concentration-
212 response data were fit by non-linear regression to a four-parameter logistic equation.
213 PFOS potency was expressed as the half-maximal inhibitory concentration (IC₅₀).
214 Statistical differences between treatment groups were determined by ANOVA followed by
215 Dunnett's multiple comparison tests.

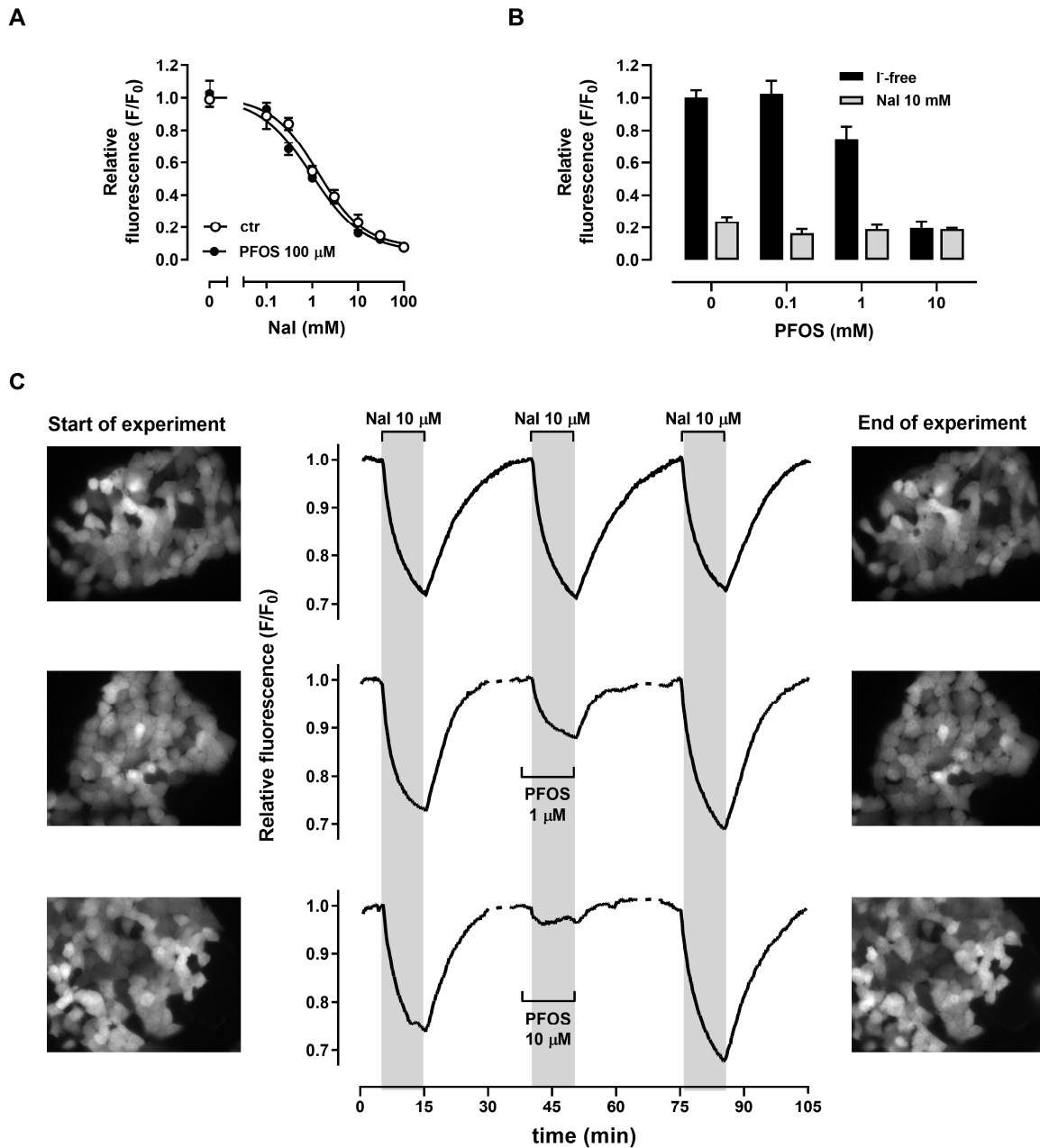
216 **3. Results**

217 **3.1. Effects of PFOS and PFOA on iodide accumulation in FRTL-5 thyroid cells**

218 YFP-H148Q/I152L was used as an iodide biosensor in FRTL-5 thyroid cells. To exclude
219 the possibility that PFOS may interfere with the fluorophore's ability to detect iodide, its
220 effect on YFP-H148Q/I152L fluorescence was first measured in a cellular extract following
221 lysis of FTRL5-YFP cells. PFOS (100 μ M) had no effect on the fluorescence intensity of
222 FRTL5-YFP extracts, nor did it alter the sensitivity of YFP-H148Q/I152L to NaI ($K_{0.5} = 1.3$
223 vs. 1.0 mM in the absence and presence of PFOS respectively, $n=4$) (Figure 1A). Higher
224 concentrations of PFOS than those used for functional studies (1-10 mM) reduced the
225 fluorescence of FRTL5-YFP extracts, suggesting a direct interaction of PFOS with the
226 fluorophore at such high concentrations (Figure 1 B).

227 Perfusion of intact FRTL5-YFP cells with 10 μ M NaI resulted in a rapid decline in cellular
228 fluorescence that was both reversible and reproducible over time (Figure 1 C). We have
229 previously demonstrated this response to be due to cellular uptake of iodide via the
230 transporter NIS (Rhoden et al., 2007). The response to NaI was diminished in the
231 presence of 1 or 10 μ M PFOS but was fully restored following removal of PFOS from the
232 perfusate (Figure 1 C). Baseline cellular fluorescence was not affected by PFOS, nor was
233 cellular morphology altered from the beginning to the end of experiments lasting up to 1 h.
234 A higher concentration of PFOS (100 μ M) caused some cells (<10%) to detach from
235 coverslips during a 10 min exposure period.

236



237

238

239

240

241

242

243

244

245

246

247

Figure 1. Effect of PFOS on YFP-H148Q/I152L fluorescence of FRTL5-YFP cells. (A) Fluorescence intensity of cellular extracts in the absence/presence of 100 μM PFOS and 0.1-100 mM Nal. (B) Fluorescence intensity of cellular extracts in the absence/presence of 10 mM Nal and 0.1-10 mM PFOS. (C) Representative tracings of YFP-H148Q/I152L fluorescence in living cells exposed to Nal and PFOS, and corresponding images captured at the beginning (left) and end (right) of each experiment. Repeated exposure of cells to 10 μM Nal induced reproducible changes in fluorescence intensity (upper tracing), with recovery of resting fluorescence between each exposure. Nal-induced fluorescence changes were reduced in the presence of 1 μM PFOS (middle tracing) or 10 μM PFOS (lower tracing) and were restored following PFOS washout. Symbols and bars in A and B represent mean ± SEM of n=4 replicates.

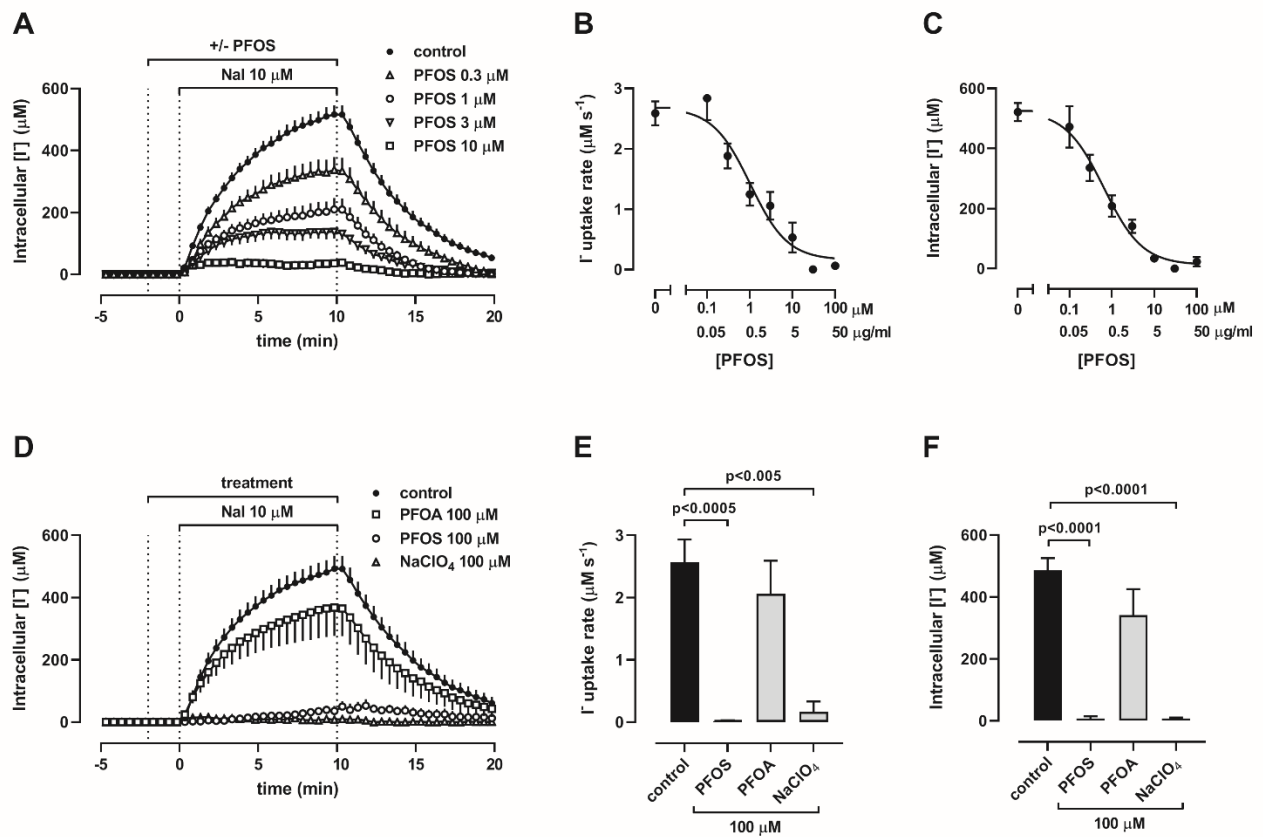
248 Intracellular iodide concentration in FRTL5-YFP cells was estimated from Nal-induced
249 changes fluorescence intensity. Consistent with the known ability of NIS to concentrate
250 iodide within thyroid cells (Portulano et al., 2014), exposure to 10 μM Nal resulted in a
251 rapid increase in intracellular iodide concentration, reaching close to 500 μM within 10 min
252 (Figure 2 A). PFOS (0.1-100 μM), added 2 min before and during Nal perfusion (Protocol
253 I), caused a concentration-dependent decrease in iodide uptake (Figure 2 A-C). The
254 concentration-dependence of PFOS obeyed a log sigmoidal relationship relative to both
255 the maximal rate of iodide uptake ($\max \Delta[\text{I}^-]/\Delta t$) and the concentration of intracellular iodide
256 reached after 10 min of perfusion with Nal ($[\text{I}^-]_{10\text{min}}$). Thus, PFOS inhibited iodide uptake
257 with an IC_{50} value of 1.0 μM ($\log \text{IC}_{50} -5.99 \pm 0.20$) and Hill slope of -0.99 for $\Delta[\text{I}^-]/\Delta t$, and
258 an IC_{50} value of 0.65 μM ($\log \text{IC}_{50} -6.19 \pm 0.16$) and Hill slope of -0.96 for $[\text{I}^-]_{10\text{min}}$ (n=6-9).
259 The lowest concentration of PFOS causing a detectable decrease in intracellular iodide
260 concentration was 0.3 μM or 150 ng/ml ($p < 0.05$ Dunnett's multiple comparison test versus
261 no PFOS control). At the highest concentration used (100 μM or 50 $\mu\text{g/ml}$), PFOS caused
262 a near-complete (>95%) inhibition of iodide uptake, as did the NIS inhibitor NaClO_4 (Figure
263 2 D-F). In contrast, PFOA (100 μM , 41 $\mu\text{g/ml}$) had no significant effect on iodide uptake
264 (Figure 2 D-F).

265

266

267

268



269

270 **Figure 2.** PFOS, but not PFOA, decreases iodide uptake by FRTL5-YFP cells. Cells were exposed
 271 to PFOS, PFOA or NaClO_4 , added 2 min before and during exposure to $10 \mu\text{M}$ Nal for a further 10
 272 min. Graphs A-C show the effects of PFOS (0.1-100 μM) on (A) the time-course of iodide uptake,
 273 (B) the maximal rate of iodide uptake, and (C) the intracellular iodide concentration at $t=10$ min.
 274 Graphs D-E show the effects of $100 \mu\text{M}$ PFOS, PFOA or NaClO_4 on (D) the time-course of iodide
 275 uptake, (E) the maximal rate of iodide uptake, and (F) the intracellular iodide concentration at $t=10$
 276 min. Symbols and bars represent mean \pm SEM of $n=6-9$ experiments.

277

278

279

280

281

282 PFOS was also able to reduce iodide concentration in iodide-containing FRT5-YFP cells,
283 evidenced as a reversal of Nal-induced fluorescence changes (Figure 3 A). In this case,
284 cells were first exposed to 10 μ M Nal for 10 min to pre-load them with iodide, followed by
285 PFOS in the continued presence of Nal for a further 10 min (Protocol II). To control for
286 differences in iodide uptake between replicate experiments that could mask the effect of
287 PFOS, intracellular iodide concentration in each experiment was normalized to the level
288 reached after 10 min of iodide uptake, immediately before PFOS addition (i.e. $[I^-]_{10\text{min}}$ is
289 defined as 100%). PFOS caused a time- and concentration-dependent decrease in iodide
290 concentration (Figures 3 B-C), with an IC_{50} of 0.92 μ M (log IC_{50} -6.04 +/- 0.14) and Hill
291 slope of -0.94 (n=4-8). The effect of PFOS (100 μ M) mimicked that of $NaClO_4$ (100 μ M),
292 whereas PFOA (100 μ M) had no significant effect (Figures 3 D-E).

293 To determine whether altered sodium gradients could contribute to PFOS-induced
294 responses, the effect of the Na-K ATPase inhibitor ouabain (100 μ M) on intracellular iodide
295 concentration was also examined (Protocol II). Compared to the time control, ouabain
296 reduced intracellular iodide concentration in iodide-containing cells by only 23% (figure 4
297 A), in contrast to the 82% inhibition induced by 10 μ M PFOS over the same 10 min time
298 frame (from figure 3 B).

299 To determine whether PFOS stimulates iodide efflux, FRTL5-YFP cells were exposed to
300 10 μ M Nal for 10 min to pre-load them with iodide, followed by washout in Nal-free BSS
301 with or without 10 μ M PFOS (Protocol III). Intracellular iodide concentration decreased
302 upon Nal-removal with a similar rate constant in the presence ($0.014 \pm 0.001 \text{ s}^{-1}$) and
303 absence ($0.012 \pm 0.002 \text{ s}^{-1}$) of PFOS (figure 4 B).

304

305
 306
 307
 308
 309
 310
 311
 312
 313
 314
 315
 316
 317
 318
 319
 320
 321
 322
 323
 324
 325
 326
 327
 328

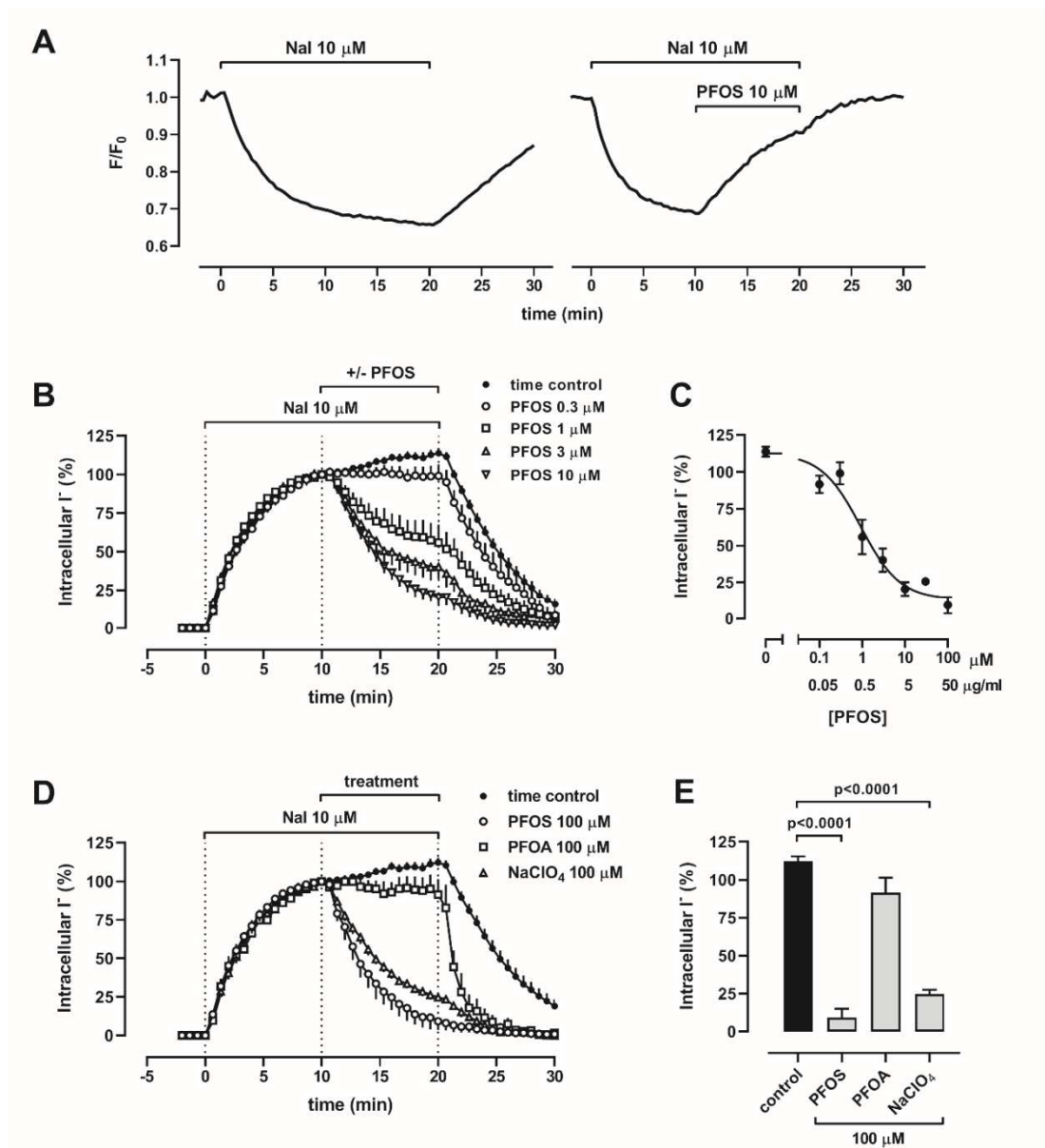


Figure 3. PFOS, but not PFOA, decreases iodide concentration in iodide-containing FRTL5-YFP cells. Cells were exposed to 10 μM Nal for 10 min, followed by 10 μM Nal +/- PFOS, PFOA or NaClO_4 for a further 10 min. (A) Representative tracing of normalized YFP-H148Q/I152L fluorescence (F/F_0). (B) Time-dependent changes in intracellular iodide concentration induced by 0-10 μM PFOS. (C) PFOS concentration-dependence of intracellular iodide concentration measured at $t=20$ min. (D) Time-dependent changes in intracellular iodide concentration induced by 100 μM PFOS, PFOA or NaClO_4 . (E) Effect of 100 μM PFOS, PFOA and NaClO_4 on intracellular iodide concentration measured at $t=20$ min. In graphs B-E, intracellular iodide concentration was normalized within each individual experiment to the level reached after 10 min of uptake, before the addition of test agents. Symbols and bars represent mean \pm SEM of $n=4-8$ experiments.

329
330
331
332
333
334
335
336
337
338
339
340
341
342
343
344
345
346
347
348
349
350
351
352
353
354

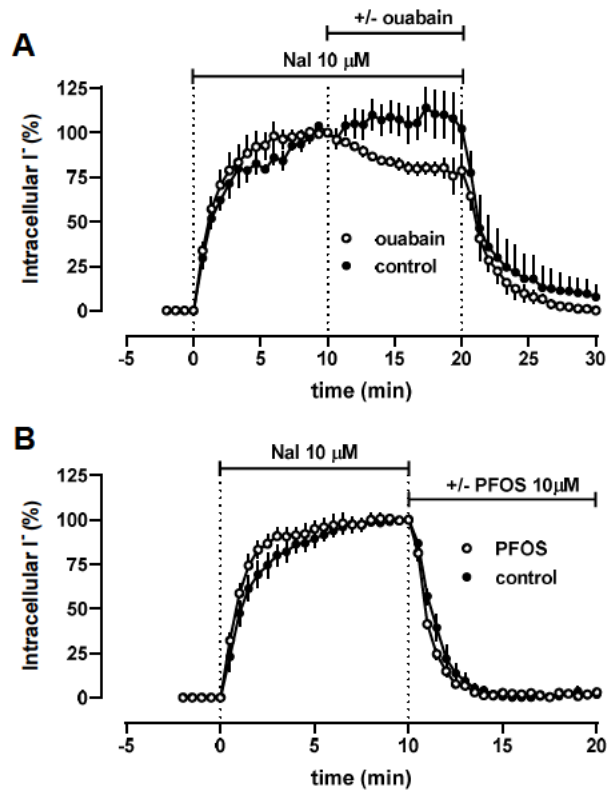


Figure 4. Effect of ouabain and PFOS on intracellular iodide concentration in FRTL5-YFP cells. (A) Cells were exposed to 10 μM Nal for 10 min, followed by 10 μM Nal +/- 100 μM ouabain for a further 10 min. (B) Cells were exposed to 10 μM Nal for 10 min, followed by Nal-free BSS +/- 10 μM PFOS for a further 10 min. Intracellular iodide concentration was normalized within each individual experiment to the level reached after 10 min of uptake, before the addition of test agents. Symbols and bars represent mean \pm SEM of n=4 experiments.

355 **3.2. Effect of PFOS on iodide accumulation in HEK-293 expressing hNIS**

356 hNIS expression in HEK-293 cells transfected with hNIS cDNA was confirmed by Western
357 blotting (Figure 5 A). NaI (10 μ M) decreased the cellular fluorescence of HEK293-YFP-
358 hNIS cells by 25% over 10 min but had a negligible (<2%) effect on HEK293-YFP cells,
359 consistent with NIS-mediated iodide uptake in the former (Figure 5 B). PFOS (10 μ M) did
360 not alter baseline fluorescence in either cell model, but reduced fluorescence changes
361 induced by NaI in HEK293-YFP-hNIS cells. This effect was reversible, with full recovery of
362 NaI-induced responses following washing with physiological solution. PFOS (10 μ M) also
363 provoked the loss of iodide from iodide-containing HEK293-YFP-hNIS cells, as indicated
364 by the reversal of NaI-induced fluorescence changes. Quantitation of intracellular iodide
365 (Figure 5 C-D) revealed a significant inhibition of iodide uptake by 10 μ M but not 1 μ M
366 PFOS, in terms of both the maximal rate of iodide uptake and the near steady-state
367 concentration reached after 10 min exposure to NaI.

368 **3.3 Effect of PFOS and PFOA on cell viability**

369 Cell viability of FRTL-5 cells exposed to 1-100 μ M PFOS or PFOA for 1h was assessed
370 using a tetrazolium-based assay (Figure 6). Although one-way ANOVA indicated an
371 overall difference ($p < 0.05$) for both compounds, Dunnett's multiple comparisons post-tests
372 failed to reveal any significant differences in the viability of cells exposed to either
373 compound compared to the time control. Tukey's multiple comparison test only revealed a
374 significant decrease in the viability of cells exposed to 100 μ M versus 30 μ M PFOS
375 ($p < 0.05$).

376

377

378

379

380

381

382

383

384

385

386

387

388

389

390

391

392

393

394

395

396

397

398

399

400

401

402

403

404

405

406

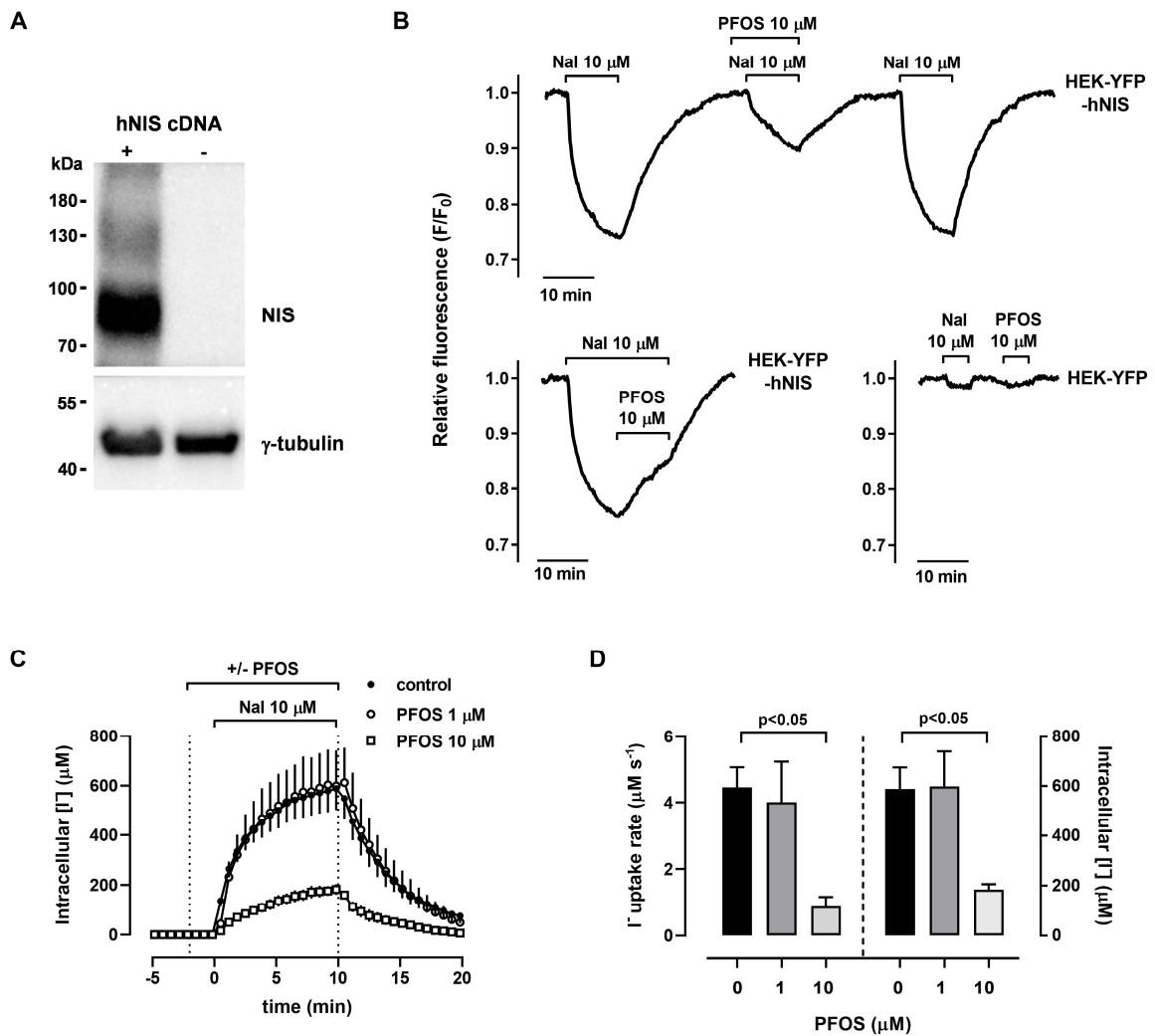


Figure 5. PFOS decreases iodide accumulation by HEK293 cells expressing hNIS. (A) Western blot detection of hNIS and γ -tubulin (loading control) in HEK-293 cell lysates (40 μ g protein), 48h after transfection with/without hNIS cDNA. (B) Representative tracings of normalized YFP-H148Q/I152L fluorescence (F/F_0) in HEK293-YFP-hNIS and HEK293-YFP cells exposed to 10 μ M Nal and/or 10 μ M PFOS. (C) Time course of iodide uptake in HEK293-YFP-hNIS in the presence of 0, 1, or 10 μ M PFOS. (D) Effect of PFOS on the maximal rate of iodide uptake and intracellular iodide concentration at t=10 min in HEK293-YFP-hNIS cells. Symbols and bars represent mean \pm SEM of n=4 experiments.

407

408

409

410

411

412

413

414

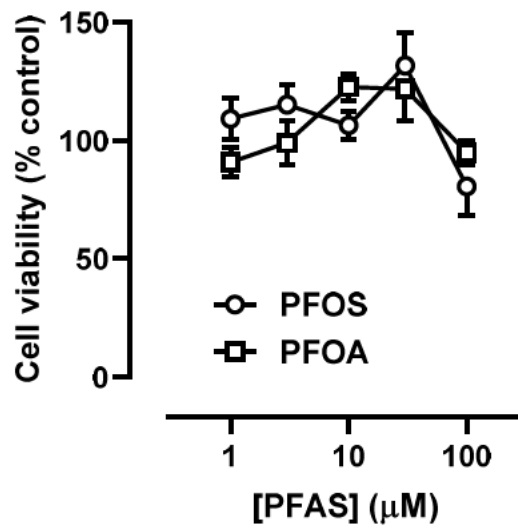
415

416

417 **Figure 6.** Effect of PFOS and PFOA on cell viability in FRTL.5 cells. Cells were exposed to PFOS
418 or PFOA for 1 h, after which cell viability was measured with a tetrazolium-based assay. Symbols
419 and bars represent mean \pm SEM of n=3-4 replicates.

420

421



422 **4. Discussion**

423 Cell-based assays are useful tools to investigate the mechanisms by which environmental
424 contaminants disrupt physiological processes. Current screening assays for NIS inhibitors
425 include radiotracer and chemical assays (Hallinger et al., 2017; Lecat-Guillet et al., 2007;
426 Waltz et al., 2010), both of which provide end-point measurements of iodide uptake by
427 NIS-expressing cells. In this study, we used a genetically encoded halide-sensitive
428 biosensor, YFP-H148Q/I152L, to monitor intracellular iodide concentration by live cell
429 imaging (Rhoden et al., 2008, 2007). Iodide quenching of cellular YFP-H148Q/I152L
430 fluorescence is rapid, reversible, and concentration-dependent. The assay requires small
431 numbers of cells and can be used to follow the time course of iodide influx and efflux in a
432 single experiment. Cells can be repeatedly exposed to extracellular iodide, with
433 reproducible changes in YFP-H148Q/I152L fluorescence. Although the technique suffers
434 some limitations (e.g. interference by intracellular pH, not suitable for difficult-to-transfect
435 cells), it is particularly useful to study the disruption of iodide homeostasis by EDCs.

436 The results of this study demonstrate that PFOS inhibits NIS-mediated iodide
437 accumulation in thyroid follicular cells, as well as in non-thyroid cells with heterologous NIS
438 expression. PFOS mimicked the NIS inhibitor perchlorate in its ability to both prevent
439 iodide uptake by cells and reduce iodide concentration in iodide-containing cells. In the
440 intact thyroid gland, the polarized expression of transport proteins on follicular cells – NIS
441 on the basolateral surface, pendrin, anoctamin-1 and possibly other channels on the apical
442 surface – normally ensures the unidirectional flow of iodide towards the follicular lumen for
443 subsequent oxidation and organification. In contrast, FRTL-5 cells are neither polarized
444 nor able to organify iodide. Since the electrochemical gradient for iodide is strongly
445 outward, NIS inhibition will cause net loss from iodide-containing cells, even in the
446 continued presence of extracellular iodide. PFOS did not alter the rate constant for iodide

447 efflux, suggesting that the decrease in intracellular iodide concentration induced by PFOS
448 is due only to inhibition of NIS-mediated uptake, and not the activation of efflux
449 channels/transporters.

450 PFOS inhibited iodide accumulation by FRTL-5 cells with an IC_{50} close to 1 μ M (log IC_{50}
451 values of -5.99 for the maximal rate of uptake $\Delta[I^-]/\Delta t$, and -6.19 for the concentration of
452 intracellular iodide reached after 10 min of perfusion with NaI), similar to the value
453 obtained for perchlorate in these cells using the same YFP-based assay (Cianchetta et al.,
454 2010). Several small monovalent anions have been shown to inhibit NIS competitively,
455 with an order of potency of $PF_6^- > ClO_4^- > BF_4^- > SCN^- \gg NO_3^- = ClO_3^- > IO_4^- \gg Br^-$
456 (Hallinger et al., 2017; Jones et al., 1996; Lecat-Guillet et al., 2007; Tonacchera et al.,
457 2004; Van Sande et al., 2003). Using a high throughput assay, the U.S. EPA's Endocrine
458 Disruptor Screening Program (EDSP) recently demonstrated that PFOS inhibits
459 radioiodide uptake in HEK-293T cells expressing human NIS, but with a more than 10-fold
460 lower potency (log IC_{50} -4.66 to -4.78) (Wang et al., 2019, 2018). In a further study, EDSP
461 reported inhibition of radioiodide uptake in FRTL-5 cells and hNIS-expressing HEK-293T
462 cells by PFOS, with log IC_{50} values of -6.45 and -5.87, respectively (Buckalew et al.,
463 2020). Different potencies may reflect the choice of cell model (heterologous versus
464 endogenous NIS expression), species (human versus rat NIS), detection method
465 (radiotracer versus fluorescent biosensor), and/or other aspects of the experimental
466 protocol (e.g. duration, iodide concentration, and temperature). .

467 PFOA, in contrast to PFOS, had no effect on iodide uptake by thyroid cells. EDSP also
468 found no effect of PFOA on radioiodide uptake in NIS-expressing HEK-293T cells (Wang
469 et al., 2019). Both compounds belong to the perfluoroalkyl acid class of PFAS that consist
470 of a fluorinated carbon chain of variable length attached to a charged functional group
471 (ITRC, 2018). PFOS ($C_8F_{17}SO_3H$) has 8 perfluorinated carbons and a sulfonic acid head,

472 whereas PFOA ($C_7F_{15}COOH$) has 7 perfluorinated carbons and a carboxylic acid head
473 (ITRC, 2018). Due to their low pK_a , PFOS and PFOA are almost completely ionized at
474 physiological pH, existing in most biologic matrices as perfluorooctane sulfonate
475 ($C_8F_{17}SO_3^-$) and perfluorooctane caboxylate ($C_7F_{15}CO_2^-$) respectively. It is therefore
476 tempting to speculate that inhibition of iodide uptake by PFOS, but not PFOA, may reflect
477 the activity of the perfluoroalkyl sulfonate but not the carboxylate anion, or may be related
478 to the length of the perfluorinated carbon chain.

479 The mechanism of NIS inhibition by PFOS is unclear. Indirect effects on cell viability or
480 sodium gradients are unlikely to play a major role, if any, since (i) cytotoxicity was not
481 observed at PFOS concentrations lower than 100 μM , and (ii) the Na-K ATPase inhibitor
482 ouabain only reduced intracellular iodide concentration by 23%, compared to the 82%
483 reduction caused by 10 μM PFOS over the same time frame. Alternatively, inhibition of
484 NIS activity by PFOS may involve direct binding to NIS and/or an interaction with NIS's
485 phospholipid environment. PFAS are known to bind proteins and to partition into
486 phospholipid bilayers, both properties contributing to their bioaccumulation (Ng and
487 Hungerbühler, 2014). Our results indicate that NIS inhibition by PFOS involves reversible
488 single-site binding, suggested by Hill slope estimates close to one, and by the complete
489 restoration of iodide uptake following PFOS washout. Further studies that assess the
490 structure-activity relationship of perfluoroalkyl anions as NIS inhibitors, with reference to
491 the functional group and the length of the fluorocarbon chain, could shed light on the
492 mechanism of NIS inhibition by PFOS.

493 Small competitive anionic NIS inhibitors, such as perchlorate, thiocyanate and nitrate, are
494 transported by NIS (Portulano et al., 2014), and are concentrated within thyroid follicular
495 cells (Di Bernardo et al., 2011; Wolff, 1964). PFOS is known to be a substrate for other
496 SLC transporters that contribute to its hepatic accumulation, renal clearance and placental

497 transfer (Kummu et al., 2015; Zhao et al., 2017, 2015). Although field and laboratory
498 studies have identified PFAAs in thyroid tissue of several mammalian and non-mammalian
499 species, there is no evidence for active or preferential accumulation in the thyroid gland
500 compared to other tissues (Maestri et al., 2006; Ng and Hungerbühler, 2014). Coperchini
501 et al. (2015) detected PFOS and PFOA in cellular pellets of FRTL-5 thyrocytes grown in
502 the presence of these compounds, and proposed a gradient-based passive diffusion
503 mechanism. In other cell types, PFAA accumulation correlates with phospholipophilicity,
504 suggesting that binding to membrane phospholipids may be the most important factor
505 driving cellular accumulation (Sanchez Garcia et al., 2018). We propose that although
506 PFOS interacts with NIS and/or its environment to inhibit iodide transport, it is not
507 necessarily transported by NIS into cells because of its size or other physicochemical
508 properties.

509 The lowest concentration of PFOS to inhibit iodide uptake in FRTL-5 thyroid cells was 0.3
510 μM (150 ng/ml), a concentration that is only observed in human serum following extreme
511 exposures. PFOS has been detected in the blood of most individuals tested in
512 industrialized nations as a result of occupational, domestic or other accidental exposure.
513 Average serum PFOS levels in the general population are typically <1-30 ng/ml, with
514 maximum individual values occasionally reaching into the 100-1000 ng/ml range (Antonia
515 M Calafat et al., 2007; Antonia M. Calafat et al., 2007; Kannan et al., 2004; Li et al., 2017;
516 Olsen et al., 2003). Thanks to regulatory interventions and voluntary industrial efforts to
517 limit PFAS production, serum PFOS levels in the general population are gradually
518 declining in many countries (Glynn et al., 2012; Kato et al., 2011; Toms et al., 2014).
519 Nevertheless, the widespread use of manufactured goods containing PFAS can result in
520 unexpectedly high exposure levels. High serum PFOS levels (median 345 ng/ml, range
521 24-1500 ng/ml) were detected in people exposed to contaminated municipal drinking

522 water, due to the use fire-fighting foams in a nearby military airfield (Li et al., 2018). In a
523 Canadian family, moderately high levels of serum PFOS (range 15.2–108 ng/ml) were
524 linked to dust ingestion and/or inhalation following home carpet treatment with
525 Scotchguard formulations (Beesoon et al., 2012). Although the present study suggests that
526 PFOS inhibits NIS at concentrations that may be relevant during exceptionally high *in vivo*
527 exposures, an important caveat for the interpretation of the inhibitory concentrations we
528 report, is the absence serum during *in vitro* exposures. It remains to be determined
529 whether binding to serum proteins such as albumin may alter the potency of PFOS as a
530 NIS inhibitor.

531 Epidemiologic and clinical data on the effects of PFAS exposure on thyroid disease risk
532 and thyroid hormone levels are mixed and often inconclusive (reviewed by Coperchini et
533 al., 2017; EFSA, 2018; USEPA, 2016). NHANES studies reported gender-dependent
534 associations of serum PFOS and/or PFOA with treated or subclinical thyroid disease in the
535 US adult population (Melzer et al., 2010; Wen et al., 2013). An association between serum
536 PFAS levels and thyroid disease was also found in exposed chemical plant workers and
537 nearby community residents (Winqvist and Steenland, 2014), but not in another population
538 exposed to high PFAS levels through contaminated municipal drinking water (Andersson
539 et al., 2019). PFAS levels show positive/negative, null or ambiguous associations with
540 TSH and thyroid hormone levels in several types of populations including exposed
541 individuals, the general population, pregnant women and mother-infant pairs (Berg et al.,
542 2015; Blake et al., 2018; Inoue et al., 2019; Li et al., 2017; Seo et al., 2018; Tsai et al.,
543 2017). The lack of consensus may reflect differences in study design, population
544 characteristics (size, developmental stage, gender, ethnicity), thyroid status (undiagnosed
545 thyroid disease, iodine sufficiency), and exposure (concentration, duration, mixture
546 effects). In fact, people are exposed to complex mixtures of PFAS present in the

547 environment, as well as other endocrine disruptors and stressors targeting the HPT axis at
548 different levels. Webster et al. proposed a “multiple hit hypothesis,” postulating that
549 individuals with multiple thyroid stressors (e.g. pregnancy, low iodine, thyroid antibodies),
550 may be more susceptible to PFAS-induced thyroid disruption. (Webster et al., 2016, 2014).
551 Thus, in pregnant women, serum PFAS levels were positively associated with TSH and
552 negatively associated with free T4, but only in women with high levels of thyroid
553 peroxidase antibodies (TPOAb) suggestive of auto-immune thyroid disease (Webster et
554 al., 2014). Furthermore, in the US adult population, associations between serum PFAS
555 and thyroid parameters occurred only those with high TPOAb and low iodine status
556 (Webster et al., 2016). Recent studies have also addressed the combined effects of
557 multiple PFAS in pregnant women, finding either positive or limited associations of PFAS
558 mixtures with thyroid hormones in maternal and cord sera (Lebeaux et al., 2020; Preston
559 et al., 2020).

560 *In vivo* studies in rats have shown that PFOS decreases circulating thyroid hormone levels
561 without changing TSH (reviewed in Coperchini et al., 2017). This is contrary to the
562 expected hypothyroid effect of NIS inhibition, such as that induced by perchlorate
563 (Männistö et al., 1979). Several mechanisms for PFOS-induced hypothyroxemia have
564 been proposed, including competitive binding to thyroid hormone transport proteins,
565 increased conversion of thyroxine (T4) to triiodothyronine (T3) by type 1 deiodinase (Yu et
566 al., 2009), and increased hepatic clearance (Coperchini et al., 2017; Yu et al., 2009).
567 Furthermore, our study evaluated acute, but not long-term, effects of PFOS/PFOA on NIS-
568 mediated iodide accumulation in thyroid cells. Chronic PFOS exposure had no effect on
569 NIS mRNA levels in rats (Yu et al., 2009), but increased them in zebrafish larvae (Shi et
570 al., 2009). Further studies to evaluate the long-term effects of PFAS on NIS expression,

571 localization and function, at concentrations that mirror serum levels, will be critical to
572 extrapolate *in vitro* findings to the interpretation of *in vivo* responses.

573 **5. Conclusion**

574 Although PFAS disruption of thyroid function is still controversial, potential effects may
575 occur through a multitude of mechanisms. Using a cell-based fluorescence assay, we
576 have shown that PFOS inhibits NIS-mediated iodide uptake by thyroid cells *in vitro*.
577 Although inhibition occurs at PFOS concentrations that are unlikely to impact the general
578 population, it may be relevant in susceptible individuals accidentally exposed to
579 exceptionally high levels. Mechanisms other than NIS inhibition may be involved in thyroid
580 disruption by PFOA. Despite the gradual phase-out of PFOS and PFOA from industrial
581 and commercial applications, the widespread use and persistence of PFAS in the human
582 habitat highlights the need for further studies to address the health effects of this important
583 class of anthropogenic chemicals.

584

585 **6. Acknowledgments**

586 This study was supported by Italy's Ministry of Health grant [RF-2011-02350857] and
587 University of Bologna intramural funds.

588 **7. Author contributions**

589 AC: Data curation; Formal analysis; Investigation; Methodology; Supervision; Writing -
590 review & editing. CS: Investigation; Methodology; Writing - review & editing. KJR:
591 Conceptualization; Data curation; Formal analysis; Funding acquisition; Investigation;
592 Methodology; Project administration; Resources; Supervision; Visualization; Roles/Writing
593 - original draft; Writing - review & editing.

594

595 **8. References**

- 596 Ambesi-Impiombato, F.S., Parks, L.A., Coon, H.G., 1980. Culture of hormone-dependent
597 functional epithelial cells from rat thyroids. *Proc. Natl. Acad. Sci. U. S. A.* 77, 3455–9.
598 <https://doi.org/10.1073/pnas.77.6.3455>
- 599 Andersson, E.M., Scott, K., Xu, Y., Li, Y., Olsson, D.S., Fletcher, T., Jakobsson, K., 2019.
600 High exposure to perfluorinated compounds in drinking water and thyroid disease. A
601 cohort study from Ronneby, Sweden. *Environ. Res.* 176, 108540.
602 <https://doi.org/10.1016/j.envres.2019.108540>
- 603 Beeson, S., Genuis, S.J., Benskin, J.P., Martin, J.W., 2012. Exceptionally high serum
604 concentrations of perfluorohexanesulfonate in a Canadian family are linked to home
605 carpet treatment applications. *Environ. Sci. Technol.* 46, 12960–7.
606 <https://doi.org/10.1021/es3034654>
- 607 Berg, V., Nøst, T.H., Hansen, S., Elverland, A., Veyhe, A.S., Jorde, R., Odland, J.Ø.,
608 Sandanger, T.M., 2015. Assessing the relationship between perfluoroalkyl
609 substances, thyroid hormones and binding proteins in pregnant women; a longitudinal
610 mixed effects approach. *Environ. Int.* 77, 63–69.
611 <https://doi.org/10.1016/j.envint.2015.01.007>
- 612 Blake, B.E., Pinney, S.M., Hines, E.P., Fenton, S.E., Ferguson, K.K., 2018. Associations
613 between longitudinal serum perfluoroalkyl substance (PFAS) levels and measures of
614 thyroid hormone, kidney function, and body mass index in the Fernald Community
615 Cohort. *Environ. Pollut.* 242, 894–904. <https://doi.org/10.1016/j.envpol.2018.07.042>
- 616 Buckalew, A.R., Wang, J., Murr, A.S., Deisenroth, C., Stewart, W.M., Stoker, T.E., Laws,
617 S.C., 2020. Evaluation of potential sodium-iodide symporter (NIS) inhibitors using a
618 secondary Fischer rat thyroid follicular cell (FRTL-5) radioactive iodide uptake (RAIU)

619 assay. *Arch. Toxicol.* 94, 873–885. <https://doi.org/10.1007/s00204-020-02664-y>

620 Calafat, Antonia M, Kuklennyik, Z., Reidy, J.A., Caudill, S.P., Tully, J.S., Needham, L.L.,
621 2007. Serum concentrations of 11 polyfluoroalkyl compounds in the u.s. population:
622 data from the national health and nutrition examination survey (NHANES). *Environ.*
623 *Sci. Technol.* 41, 2237–42. <https://doi.org/10.1021/es062686m>

624 Calafat, Antonia M., Wong, L.Y., Kuklennyik, Z., Reidy, J.A., Needham, L.L., 2007.
625 Polyfluoroalkyl chemicals in the U.S. population: Data from the national health and
626 nutrition examination survey (NHANES) 2003-2004 and comparisons with NHANES
627 1999-2000. *Environ. Health Perspect.* 115, 1596–1602.
628 <https://doi.org/10.1289/ehp.10598>

629 Cianchetta, S., di Bernardo, J., Romeo, G., Rhoden, K.J., 2010. Perchlorate transport and
630 inhibition of the sodium iodide symporter measured with the yellow fluorescent protein
631 variant YFP-H148Q/I152L. *Toxicol. Appl. Pharmacol.* 243, 372–380.
632 <https://doi.org/10.1016/j.taap.2009.12.004>

633 Coperchini, F., Awwad, O., Rotondi, M., Santini, F., Imbriani, M., Chiovato, L., 2017.
634 Thyroid disruption by perfluorooctane sulfonate (PFOS) and perfluorooctanoate
635 (PFOA). *J. Endocrinol. Invest.* 40, 105–121. [https://doi.org/10.1007/s40618-016-0572-](https://doi.org/10.1007/s40618-016-0572-z)
636 [z](https://doi.org/10.1007/s40618-016-0572-z)

637 Coperchini, F., Pignatti, P., Lacerenza, S., Negri, S., Sideri, R., Testoni, C., de Martinis, L.,
638 Cottica, D., Magri, F., Imbriani, M., Rotondi, M., Chiovato, L., 2015. Exposure to
639 perfluorinated compounds: in vitro study on thyroid cells. *Environ. Sci. Pollut. Res.* 22,
640 2287–2294. <https://doi.org/10.1007/s11356-014-3480-9>

641 Di Bernardo, J., Iosco, C., Rhoden, K.J., 2011. Intracellular anion fluorescence assay for
642 sodium/iodide symporter substrates. *Anal. Biochem.* 415.

643 <https://doi.org/10.1016/j.ab.2011.04.017>

644 EFSA Panel on Contaminants in the Food Chain (CONTAM), Helle Katrine Knutsen, Jan
645 Alexander, Lars Barregård, Margherita Bignami, B.B., Sandra Ceccatelli, Bruce
646 Cottrill, Michael Dinovi, Lutz Edler, B.G.-K., Christer Hogstrand, Laurentius (Ron)
647 Hoogenboom, Carlo Stefano Nebbia, I.P.O., Annette Petersen, Martin Rose, Alain-
648 Claude Roudot, Christiane Vleminckx, G.V., Heather Wallace, Laurent Bodin, Jean-
649 Pierre Cravedi, T.I.H., Line Småstuen Haug, Niklas Johansson, Henk van Loveren,
650 Petra Gergelova, K.M., Sara Levorato, M. van M. and T.S., 2018. Risk to human
651 health related to the presence of perfluorooctane sulfonic acid and perfluorooctanoic
652 acid in food. *EFSA J.* 16(12), 5194.

653 Galietta, L.J.V., Haggie, P.M., Verkman, A.S., 2001. Green fluorescent protein-based
654 halide indicators with improved chloride and iodide affinities. *FEBS Lett.* 499, 220–
655 224. [https://doi.org/10.1016/S0014-5793\(01\)02561-3](https://doi.org/10.1016/S0014-5793(01)02561-3)

656 Glynn, A., Berger, U., Bignert, A., Ullah, S., Aune, M., Lignell, S., Darnerud, P.O., 2012.
657 Perfluorinated alkyl acids in blood serum from primiparous women in Sweden: serial
658 sampling during pregnancy and nursing, and temporal trends 1996-2010. *Environ.*
659 *Sci. Technol.* 46, 9071–9. <https://doi.org/10.1021/es301168c>

660 Hallinger, D.R., Murr, A.S., Buckalew, A.R., Simmons, S.O., Stoker, T.E., Laws, S.C.,
661 2017. Development of a screening approach to detect thyroid disrupting chemicals
662 that inhibit the human sodium iodide symporter (NIS). *Toxicol. Vitro.* 40, 66–78.
663 <https://doi.org/10.1016/j.tiv.2016.12.006>

664 Inoue, K., Ritz, B., Andersen, S.L., Ramlau-Hansen, C.H., Høyer, B.B., Bech, B.H.,
665 Henriksen, T.B., Bonefeld-Jørgensen, E.C., Olsen, J., Liew, Z., 2019. Perfluoroalkyl
666 substances and maternal thyroid hormones in early pregnancy; findings in the danish

667 national birth cohort. *Environ. Health Perspect.* 127, 117002.
668 <https://doi.org/10.1289/EHP5482>

669 ITRC (Interstate Technology & Regulatory Council), 2018. PFAS Fact Sheets PFAS-1,
670 Washington, D.C.: Interstate Technology & Regulatory Council, PFAS Team.
671 www.itrcweb.org.

672 Jones, P.A., Pendlington, R.U., Earl, L.K., Sharma, R.K., Barratt, M.D., 1996. In vitro
673 investigations of the direct effects of complex anions on thyroidal iodide uptake:
674 Identification of novel inhibitors. *Toxicol. Vitro.* 10, 149–160.
675 [https://doi.org/10.1016/0887-2333\(95\)00114-X](https://doi.org/10.1016/0887-2333(95)00114-X)

676 Kannan, K., Corsolini, S., Falandysz, J., Fillmann, G., Kumar, K.S., Loganathan, B.G.,
677 Mohd, M.A., Olivero, J., Van Wouwe, N., Yang, J.H., Aldoust, K.M., 2004.
678 Perfluorooctanesulfonate and related fluorochemicals in human blood from several
679 countries. *Environ. Sci. Technol.* 38, 4489–95. <https://doi.org/10.1021/es0493446>

680 Kato, K., Wong, L.Y., Jia, L.T., Kuklennyik, Z., Calafat, A.M., 2011. Trends in exposure to
681 polyfluoroalkyl chemicals in the U.S. Population: 1999-2008. *Environ. Sci. Technol.*
682 45, 8037–45. <https://doi.org/10.1021/es1043613>

683 KEMI (Swedish Chemicals Agency), 2015. Report 7/15: Occurrence and use of highly
684 fluorinated substances and alternatives, <https://www.kemi.se>.

685 Kummu, M., Sieppi, E., Koponen, J., Laatio, L., Vähäkangas, K., Kiviranta, H., Rautio, A.,
686 Myllynen, P., 2015. Organic anion transporter 4 (OAT 4) modifies placental transfer of
687 perfluorinated alkyl acids PFOS and PFOA in human placental ex vivo perfusion
688 system. *Placenta* 36, 1185–91. <https://doi.org/10.1016/j.placenta.2015.07.119>

689 Lebeaux, R.M., Doherty, B.T., Gallagher, L.G., Zoeller, R.T., Hoofnagle, A.N., Calafat,

- 690 A.M., Karagas, M.R., Yolton, K., Chen, A., Lanphear, B.P., Braun, J.M., Romano,
691 M.E., 2020. Maternal serum perfluoroalkyl substance mixtures and thyroid hormone
692 concentrations in maternal and cord sera: The HOME Study. *Environ. Res.* 185,
693 109395. <https://doi.org/10.1016/j.envres.2020.109395>
- 694 Lecat-Guillet, N., Merer, G., Lopez, R., Pourcher, T., Rousseau, B., Ambroise, Y., 2007. A
695 96-well automated radioiodide uptake assay for sodium/iodide symporter inhibitors.
696 *Assay Drug Dev. Technol.* 5, 535–40. <https://doi.org/10.1089/adt.2007.068>
- 697 Li, Y., Cheng, Y., Xie, Z., Zeng, F., 2017. Perfluorinated alkyl substances in serum of the
698 southern Chinese general population and potential impact on thyroid hormones. *Sci.*
699 *Rep.* 7, 43380. <https://doi.org/10.1038/srep43380>
- 700 Li, Y., Fletcher, T., Mucs, D., Scott, K., Lindh, C.H., Tallving, P., Jakobsson, K., 2018. Half-
701 lives of PFOS, PFHxS and PFOA after end of exposure to contaminated drinking
702 water. *Occup. Environ. Med.* 75, 46–51. <https://doi.org/10.1136/oemed-2017-104651>
- 703 Maestri, L., Negri, S., Ferrari, M., Ghittori, S., Fabris, F., Danesino, P., Imbriani, M., 2006.
704 Determination of perfluorooctanoic acid and perfluorooctanesulfonate in human
705 tissues by liquid chromatography/single quadrupole mass spectrometry. *Rapid*
706 *Commun. Mass Spectrom.* 20, 2728–2734. <https://doi.org/10.1002/rcm.2661>
- 707 Männistö, P.T., Ranta, T., Leppäluoto, J., 1979. Effects of methylmercaptoimidazole
708 (MMI), propylthiouracil (PTU), potassium perchlorate (KClO₄) and potassium iodide
709 (KI) on the serum concentrations of thyrotrophin (TSH) and thyroid hormones in the
710 rat. *Acta Endocrinol. (Copenh.)* 91, 271–81. <https://doi.org/10.1530/acta.0.0910271>
- 711 Melzer, D., Rice, N., Depledge, M.H., Henley, W.E., Galloway, T.S., 2010. Association
712 between serum perfluorooctanoic acid (PFOA) and thyroid disease in the U.S.
713 National Health and Nutrition Examination Survey. *Environ. Health Perspect.* 118,

714 686–92. <https://doi.org/10.1289/ehp.0901584>

715 Ng, C.A., Hungerbühler, K., 2014. Bioaccumulation of Perfluorinated Alkyl Acids:
716 Observations and Models. *Environ. Sci. Technol.* 48, 4637–4648.
717 <https://doi.org/10.1021/es404008g>

718 Olsen, G.W., Burris, J.M., Ehresman, D.J., Froehlich, J.W., Seacat, A.M., Butenhoff, J.L.,
719 Zobel, L.R., 2007. Half-life of serum elimination of perfluorooctanesulfonate,
720 perfluorohexanesulfonate, and perfluorooctanoate in retired fluorochemical production
721 workers. *Environ. Health Perspect.* 115, 1298–305. <https://doi.org/10.1289/ehp.10009>

722 Olsen, G.W., Church, T.R., Miller, J.P., Burris, J.M., Hansen, K.J., Lundberg, J.K.,
723 Armitage, J.B., Herron, R.M., Medhdizadehkashi, Z., Nobiletti, J.B., O'Neill, E.M.,
724 Mandel, J.H., Zobel, L.R., 2003. Perfluorooctanesulfonate and other fluorochemicals
725 in the serum of American Red Cross adult blood donors. *Environ. Health Perspect.*
726 111, 1892–1901. <https://doi.org/10.1289/ehp.6316>

727 Portulano, C., Paroder-Belenitsky, M., Carrasco, N., 2014. The Na⁺/I⁻ symporter (NIS):
728 mechanism and medical impact. *Endocr. Rev.* 35, 106–49.
729 <https://doi.org/10.1210/er.2012-1036>

730 Preston, E. V., Webster, T.F., Claus Henn, B., McClean, M.D., Gennings, C., Oken, E.,
731 Rifas-Shiman, S.L., Pearce, E.N., Calafat, A.M., Fleisch, A.F., Sagiv, S.K., 2020.
732 Prenatal exposure to per- and polyfluoroalkyl substances and maternal and neonatal
733 thyroid function in the Project Viva Cohort: A mixtures approach. *Environ. Int.* 139,
734 105728. <https://doi.org/10.1016/j.envint.2020.105728>

735 Rhoden, K.J., Cianchetta, S., Duchi, S., Romeo, G., 2008. Fluorescence quantitation of
736 thyrocyte iodide accumulation with the yellow fluorescent protein variant YFP-
737 H148Q/I152L. *Anal. Biochem.* 373, 239–246. <https://doi.org/10.1016/j.ab.2007.10.020>

- 738 Rhoden, K.J., Cianchetta, S., Stivani, V., Portulano, C., Galiotta, L.J. V, Romeo, G., 2007.
739 Cell-based imaging of sodium iodide symporter activity with the yellow fluorescent
740 protein variant YFP-H148Q/I152L. *Am. J. Physiol. Cell Physiol.* 292, C814-23.
741 <https://doi.org/10.1152/ajpcell.00291.2006>
- 742 Sanchez Garcia, D., Sjödin, M., Hellstrandh, M., Norinder, U., Nikiforova, V., Lindberg, J.,
743 Wincent, E., Bergman, Å., Cotgreave, I., Munic Kos, V., 2018. Cellular accumulation
744 and lipid binding of perfluorinated alkylated substances (PFASs) - A comparison with
745 lysosomotropic drugs. *Chem. Biol. Interact.* 281, 1–10.
746 <https://doi.org/10.1016/j.cbi.2017.12.021>
- 747 Seo, S.H., Son, M.H., Choi, S.D., Lee, D.H., Chang, Y.S., 2018. Influence of exposure to
748 perfluoroalkyl substances (PFASs) on the Korean general population: 10-year trend
749 and health effects. *Environ. Int.* 113, 149–161.
750 <https://doi.org/10.1016/j.envint.2018.01.025>
- 751 Shi, X., Liu, C., Wu, G., Zhou, B., 2009. Waterborne exposure to PFOS causes disruption
752 of the hypothalamus-pituitary-thyroid axis in zebrafish larvae. *Chemosphere* 77,
753 1010–1018. <https://doi.org/10.1016/j.chemosphere.2009.07.074>
- 754 Smanik, P.A., Liu, Q., Furminger, T.L., Ryu, K., Xing, S., Mazzaferri, E.L., Jhiang, S.M.,
755 1996. Cloning of the human sodium iodide symporter. *Biochem. Biophys. Res.*
756 *Commun.* 226, 339–345. <https://doi.org/10.1006/bbrc.1996.1358>
- 757 Tazebay, U.H., Wapnir, I.L., Levy, O., Dohan, O., Zuckier, L.S., Zhao, Q.H., Deng, H.F.,
758 Amenta, P.S., Fineberg, S., Pestell, R.G., Carrasco, N., 2000. The mammary gland
759 iodide transporter is expressed during lactation and in breast cancer. *Nat. Med.* 6,
760 871–878. <https://doi.org/10.1038/78630>
- 761 Toms, L.-M.L., Thompson, J., Rotander, A., Hobson, P., Calafat, A.M., Kato, K., Ye, X.,

762 Broomhall, S., Harden, F., Mueller, J.F., 2014. Decline in perfluorooctane sulfonate
763 and perfluorooctanoate serum concentrations in an Australian population from 2002 to
764 2011. *Environ. Int.* 71, 74–80. <https://doi.org/10.1016/j.envint.2014.05.019>

765 Tonacchera, M., Pinchera, A., Dimida, A., Ferrarini, E., Agretti, P., Vitti, P., Santini, F.,
766 Crump, K., Gibbs, J., 2004. Relative potencies and additivity of perchlorate,
767 thiocyanate, nitrate, and iodide on the inhibition of radioactive iodide uptake by the
768 human sodium iodide symporter. *Thyroid* 14, 1012–9.
769 <https://doi.org/10.1089/thy.2004.14.1012>

770 Tsai, M.-S., Lin, C.-C., Chen, M.-H., Hsieh, W.-S., Chen, P.-C., 2017. Perfluoroalkyl
771 substances and thyroid hormones in cord blood. *Environ. Pollut.* 222, 543–548.
772 <https://doi.org/10.1016/j.envpol.2016.11.027>

773 USEPA (U.S. Environmental Protection Agency), 2016. Drinking Water Health Advisories
774 for PFOA and PFOS (EPA 822-R-16-002/003/004/005) [WWW Document].
775 <https://www.epa.gov>.

776 Van Sande, J., Massart, C., Beauwens, R., Schoutens, A., Costagliola, S., Dumont, J.E.,
777 Wolff, J., 2003. Anion Selectivity by the Sodium Iodide Symporter. *Endocrinology* 144,
778 247–252. <https://doi.org/10.1210/en.2002-220744>

779 Waltz, F., Pillette, L., Ambroise, Y., 2010. A nonradioactive iodide uptake assay for sodium
780 iodide symporter function. *Anal. Biochem.* 396, 91–95.
781 <https://doi.org/10.1016/j.ab.2009.08.038>

782 Wang, J., Hallinger, D.R., Murr, A.S., Buckalew, A.R., Lougee, R.R., Richard, A.M., Laws,
783 S.C., Stoker, T.E., 2019. High-throughput screening and chemotype-enrichment
784 analysis of ToxCast phase II chemicals evaluated for human sodium-iodide symporter
785 (NIS) inhibition. *Environ. Int.* 126, 377–386.

786 <https://doi.org/10.1016/j.envint.2019.02.024>

787 Wang, J., Hallinger, D.R., Murr, A.S., Buckalew, A.R., Simmons, S.O., Laws, S.C., Stoker,
788 T.E., 2018. High-Throughput Screening and Quantitative Chemical Ranking for
789 Sodium-Iodide Symporter Inhibitors in ToxCast Phase I Chemical Library. *Environ.*
790 *Sci. Technol.* 52, 5417–5426. <https://doi.org/10.1021/acs.est.7b06145>

791 Wang, Z., DeWitt, J.C., Higgins, C.P., Cousins, I.T., 2017. A Never-Ending Story of Per-
792 and Polyfluoroalkyl Substances (PFASs)? *Environ. Sci. Technol.* 51, 2508–2518.
793 <https://doi.org/10.1021/acs.est.6b04806>

794 Webster, G.M., Rauch, S.A., Marie, N.S., Mattman, A., Lanphear, B.P., Venners, S.A.,
795 2016. Cross-Sectional Associations of Serum Perfluoroalkyl Acids and Thyroid
796 Hormones in U.S. Adults: Variation According to TPOAb and Iodine Status (NHANES
797 2007-2008). *Environ. Health Perspect.* 124, 935–42.
798 <https://doi.org/10.1289/ehp.1409589>

799 Webster, G.M., Venners, S.A., Mattman, A., Martin, J.W., 2014. Associations between
800 Perfluoroalkyl acids (PFASs) and maternal thyroid hormones in early pregnancy: A
801 population-based cohort study. *Environ. Res.* 133, 338–347.
802 <https://doi.org/10.1016/j.envres.2014.06.012>

803 Wen, L.-L., Lin, L.-Y., Su, T.-C., Chen, P.-C., Lin, C.-Y., 2013. Association between serum
804 perfluorinated chemicals and thyroid function in U.S. adults: the National Health and
805 Nutrition Examination Survey 2007-2010. *J. Clin. Endocrinol. Metab.* 98, E1456-64.
806 <https://doi.org/10.1210/jc.2013-1282>

807 WHO (World Health Organization), 2013. State of the science of endocrine disrupting
808 chemicals - 2012 an assessment of the state of the science of endocrine disruptors.

809 Winquist, A., Steenland, K., 2014. Perfluorooctanoic acid exposure and thyroid disease in
810 community and worker cohorts. *Epidemiology* 25, 255–64.
811 <https://doi.org/10.1097/EDE.0000000000000040>

812 Wolff, J., 1964. Transport of Iodide and Other Anions in the Thyroid Gland. *Physiol. Rev.*
813 44, 45–90. <https://doi.org/10.1152/physrev.1964.44.1.45>

814 Yu, W.-G., Liu, W., Jin, Y.-H., 2009. Effects of perfluorooctane sulfonate on rat thyroid
815 hormone biosynthesis and metabolism. *Environ. Toxicol. Chem.* 28, 990.
816 <https://doi.org/10.1897/08-345.1>

817 Yu, W.G., Liu, W., Jin, Y.H., 2009. Effects of perfluorooctane sulfonate on RAT thyroid
818 hormone biosynthesis and metabolism. *Environ. Toxicol. Chem.* 28, 990–996.
819 <https://doi.org/10.1897/08-345.1>

820 Zhao, W., Zitzow, J.D., Ehresman, D.J., Chang, S.-C., Butenhoff, J.L., Forster, J.,
821 Hagenbuch, B., 2015. Na⁺/Taurocholate Cotransporting Polypeptide and Apical
822 Sodium-Dependent Bile Acid Transporter Are Involved in the Disposition of
823 Perfluoroalkyl Sulfonates in Humans and Rats. *Toxicol. Sci.* 146, 363–73.
824 <https://doi.org/10.1093/toxsci/kfv102>

825 Zhao, W., Zitzow, J.D., Weaver, Y., Ehresman, D.J., Chang, S.-C., Butenhoff, J.L.,
826 Hagenbuch, B., 2017. Organic Anion Transporting Polypeptides Contribute to the
827 Disposition of Perfluoroalkyl Acids in Humans and Rats. *Toxicol. Sci.* 156, 84–95.
828 <https://doi.org/10.1093/toxsci/kfw236>

829

Highlights

- Disruption of thyroid iodide homeostasis by environmental contaminants
- Intracellular iodide in thyroid cells monitored with a fluorescent biosensor
- PFOS inhibits iodide uptake in thyroid cells via the Sodium Iodide Symporter
- PFOS does not stimulate iodide efflux from thyroid cells